Electronic Supplementary Information (ESI):

Taming the challenges of activity and selectivity in the electrochemical nitrogen reduction reaction using graphdiyne-supported double-atom catalysts

Yongkang Xu,‡[a] Zhewei Cai,‡[b] Pan Du,[c] Jiaxing Zhou,[a] Yonghui Pan,[a] Ping Wu,*[a] and Chenxin Cai*[a]

[a]Jiangsu Key Laboratory of New Power Batteries, Jiangsu Collaborative Innovation Center of Biomedical Functional Materials, College of Chemistry and Materials Science, Nanjing Normal University, Nanjing 210023, P.R. China

[b]Department of Chemical and Biomolecular Engineering, Clarkson University, Potsdam, New York 13699, United States.

[c]College of Life Science and Chemistry, Jiangsu Second Normal University, Nanjing 210013, P. R. China.

* Corresponding author, E-mail: wuping@njnu.edu.cn (P. Wu); cxcai@njnu.edu.cn (C. Cai).

‡ Y. Xu and Z. Cai contributed equally this work.

Contents:

1. Calculation details

(1) Methods

All calculations were performed by using the density functional theory (DFT) method implemented in DMol^3 package.[1,2] The generalized gradient approximation combined with the Perdew, Burke, and Ernzerhof (PBE) functional was employed to describe the exchange-correlation interactions.[3] A DFT-D semiempirical correction with Grimme method (DFT-D2) is applied to account for the dispersion interaction,[4] and the density functional semicore pseudopotential (DSPP) was adopted for the relativistic effects of transition metal (TM) atoms, in which the core electrons were replaced by a single effective potential and some degree of relativistic corrections are introduced into the core.[5] The double numerical plus polarization (DNP) was chosen as the basis set for other elements (C and H atoms). To sample the Brillouin zone, Monkhorst-Pack (MP) mesh of 4 × 4 × 1 k-point grid in reciprocal space were used for free energy calculations and 8 × 8 × 1 for density of states (DOS) calculations. The real-space global cutoff radius is set to be 5.2 Å. Fermi occupation is applied to achieve electronic convergence. In all of the calculations, the convergence criteria for energy, force, and displacement were set to 10^{-5} Ha, 0.002 Ha/Å, and 0.005 Å, respectively. The charge transfer and magnetic moment were obtained based on the Hirshfeld charge analysis.

(2) Gibbs Ffree energy

The reaction free energy was calculated based on the computational hydrogen electrode (CHE) model proposed by Nørskov et al.[6] In this model, the free energy of the electron-proton pair ($H^+ + e^-$) can be referenced to the chemical potential of gaseous H_2 at equilibrium (0 V, vs standard hydrogen electrode, SHE). Accordingly, the free energy change (ΔG) of each elemental step can be calculated as follows:

$$\Delta G = \Delta E + \Delta E_{ZPE} - T\Delta S + eU + \Delta G_{pH} \qquad \text{(S1)}$$

Where ΔE is the adsorption energy of adsorbates adsorbed on the surface of catalysts, obtained from DFT calculations. ΔE_{ZPE} and $T\Delta S$ are the contributions of the changes of the zero-point energy and entropy to ΔG, respectively, which are obtained from the vibrational frequency. T is the temperature and taken as

298.15 K, and ΔS is the entropy change. The vibrational frequencies of molecules in the gas phase are taken from the NIST database,[7] and those of the adsorbed intermediates were calculated. E_{ZPE} and TS (at 298.15 K) of the intermediates adsorbed on FeM-GDYs are presented in Table S4. e and U are the number of electrons transferred and the electrode potential applied, respectively. For all the adsorbed intermediates on the FeM-GDYs, only the vibrational entropy needs to be taken into account because the translational and rotational degrees of freedom of the adsorbates effectively convert into vibrational modes. The vibrational entropy is estimated using the following equation:

$$S_{vib} = R\sum_i \frac{\frac{hv_i}{k_BT}\exp\left(-\frac{hv_i}{k_BT}\right)}{1-\exp\left(-\frac{hv_i}{k_BT}\right)} - R\sum_i \ln\left[1-\exp\left(-\frac{hv_i}{k_BT}\right)\right] \quad \text{(S2)}$$

where R, h, k_B, T, v_i are the molar gas constant, Planck's constant, Boltzmann's constant, temperature (298.15 K), and the vibrational frequency, respectively. The entropy of gas molecule (H_2, N_2, and NH_3) were taken from standard values (NIST database).[7] ΔG_{pH} is the correction of the H^+ free energy by the concentration and can be expressed as $\Delta G_{pH} = 2.303\ k_BT \times$ pH. In this work, the free energy diagrams are calculated at $U = 0$ V, and pH = 0 is assumed in an acidic medium.

(3) Reaction energy barrier

The reaction energy barrier (E_a) was investigated by using complete linear synchronous transit (LST)/quadratic synchronous transit (QST) computations.[8] The root-mean-square (RMS) convergence is set to 0.002 Ha/Å, the Max.number QST steps is set to 20, and the frequency calculation was used to determine the transition state configuration. A layer of water with a solvated proton was added on the catalyst surface to explicitly model the electrochemical solid-liquid interface and search for the transition states for all the proton transfer processes. The E_a was calculated using:

$$E_a = E_{TS} - E_{IS} \quad \text{(S3)}$$

in which E_{TS} and E_{IS} are the energy of the transition and initial states, respectively.

To obtain the correlation between the E_a and electrode potential, a so-called "charge-extrapolation" method[9,10] is employed. Based on this method, the relationship between the E_a(at U) and E_a (0 V) can be given as follows:

$$E_a(\text{at } U) = E_a(0 \text{ V}) - \Delta q\, e^- U \qquad \text{(S4)}$$

Δq is the charge differences between the TS and IS.

Assuming the work function, energy, and the interfacial charge of the IS is Φ_1, $E_1(\Phi_1)$, and q_1, respectively, the work function, energy, and the interfacial charge of the TS is Φ_2, $E_2(\Phi_2)$, and q_2, respectively. According to the method proposed by Nørskov et al.,[9,10] the corresponding energy change between IS and TS at constant work functions, Φ_1 and Φ_2, are given by:

$$E_2(\Phi_1) - E_1(\Phi_1) = E_2(\Phi_2) - E_1(\Phi_1) + \frac{(q_2 - q_1)(\Phi_2 - \Phi_1)}{2} \qquad \text{(S5)}$$

$$E_2(\Phi_2) - E_1(\Phi_2) = E_2(\Phi_2) - E_1(\Phi_1) - \frac{(q_2 - q_1)(\Phi_2 - \Phi_1)}{2} \qquad \text{(S6)}$$

Taking (S6)–(S5), and setting $\Delta E(\Phi) = E_2(\Phi) - E_1(\Phi)$ at a given work function Φ and $\Delta q = q_2 - q_1$, the equation (S7) can be obtained:

$$\Delta E(\Phi_2) - \Delta E(\Phi_1) = -\Delta q\, (\Phi_2 - \Phi_1) \qquad \text{(S7)}$$

where $\Delta E(\Phi_1)$ and $\Delta E(\Phi_2)$ represent the energy barriers at constant Φ_1 and Φ_2, respectively.

If we set the Φ_1 as the reference work function, i.e., at $U = 0$ V, the Φ_2 is the work function at specific potential, U, thus,

$$E_a \text{ (at } U) = E_a(\text{at } U = 0 \text{ V}) - \Delta q\, (\Phi_2 - \Phi_1) \qquad \text{(S8)}$$

Because $\Phi_2 - \Phi_1 = e^- \cdot U$, we obtain equation (S4).

(4) Molecular dynamic (MD) simulation

To simulate the stability of FeNi-GDY, we carry out isobaric-isothermal (NPT) ensemble molecular dynamics (MD) simulation at 500 K in which the time step was set at 2.0 fs for a total period of 10 ps in MS Forcite code.[11] The calculation quality is set to Ultra-fine, the velocity initialization is set to random

and the pressure is set to standard atmospheric pressure (101.325 kPa). The Berendsen method is used to control the temperature and pressure, and the universal force field is used for dynamic simulation.

(5) Faradaic efficiency (FE)

The FE of eNRR was calculated using the definition proposed by Yang et al.[12]

$$FE\% = \frac{1}{1 + exp(\frac{\Delta G}{k_B T})} \times 100 \quad \text{(S5)}$$

where the ΔG is the Gibbs free energy differences between the processes of the H and N_2 adsorption, i.e., $\Delta G = \Delta G(N_2) - \Delta G(H)$.

(6) H adsorption on bulk metal surface

To check whether the suppression ability of the FeM-GDYs to H adsorption is better than that of the corresponding bulk metal, the adsorption free energy of H on bulk metal surfaces, was calculated. Different surfaces were employed for different metals, for metals of Sc, Ti, Co, Y, Zr, Ru, and Hf, which have a hcp structure, the (0001) surface were used; for metals of Ni, Cu, Rh, Pd, Ir, Pt, and Mn, having fcc structures, (111) surface was used; and for the metals of V, Fe, Mo, Cr, Nb, and Ta, having bcc structures, the (110) surface was used . All flat surfaces were modeled with four layers, the two topmost layers were fully relaxed, and the two bottom layers were fixed to the bulk distances. To eliminate imaginary interactions, enough vacuum (20 Å) was added with *z*-axis for all metal surfaces. Structure relaxation and total electronic energies calculation were performed using spin-polarized density-functional theory (DFT) calculations implemented in DMol[3] code.

Reference

1 B. Delley, *J. Chem. Phys.*, 1990, **92**, 508–517.

2 B. Delley, *J. Chem. Phys.*, 2000, **113**, 7556–7664.

3 J. P. Perdew, K. Burke and M. Ernzerhof, *Phys. Rev. Lett.*, 1996, **77**, 3865–3868.

4 S. Grimme, *J. Comput. Chem.*, 2006, **27**, 1787–1799.

5 B. Delley, *Phys. Rev. B: Condens. Matter Mater. Phys.*, 2002, **66**, 155125.

6 J. K. Nørskov, J. Rossmeisl, A. Logadottir, L. Lindqvist, J. R. Kitchin, T. Bligaard and H. Jónsson, *J. Phys. Chem. B*, 2004, **108**, 17886–17892.

7 Computational chemistry comparison and benchmark database. http://cccbdb.nist.gov/.

8 N. Govind, M. Petersen, G. Fitzgerald, D. King-Smith and J. A. Andzelm, *Comput. Mater. Sci.*, 2003, **28**, 250–258.

9 K. Chan and J. K. Nørskov, *J. Phys. Chem. Lett.*, 2015, **6**, 2663–2668.

10 K. Chan and J. K. Nørskov, *J. Phys. Chem. Lett.*, 2016, **7**, 1686–1690.

11 A. K. Rappe, C. J. Casewit, K. S. Colwell, W. A. Goddard III and W. M. Skiff, *J. Am. Chem. Soc.*, 1992, **114**, 10024–10035.

12 W. Zhao, L. Zhang, Q. Luo, Z. Hu, W. Zhang, S. Smith and J. Yang, *ACS Catal.*, 2019, **9**, 3419–3425.

2. Tables

Table S1. The structural parameters of the formed FeM-GDYs.[a]

FeM-GDY	$d_{min(Fe–C)}$ (Å)	$d_{max(Fe–C)}$ (Å)	r_{Fe-C} (Å)	$d_{min(M–C)}$ (Å)	$d_{max(M–C)}$ (Å)	$r_{M–C}$ (Å)	$d_{Fe–M}$ (Å)	$r_{Fe–M}$ (Å)
FeSc-GDY	1.82	2.02	2.08	2.21	2.40	2.43	2.63	3.02
FeTi-GDY	1.88	2.05	2.08	2.13	2.32	2.33	2.46	2.92
FeV-GDY	1.86	2.04	2.08	2.07	2.23	2.26	2.46	2.85
FeCr-GDY	1.86	2.04	2.08	2.07	2.08	2.10	2.46	2.71
FeMn-GDY	1.86	2.06	2.08	2.01	2.06	2.10	2.48	2.71
FeFe-GDY	1.88	1.97	2.08	1.91	2.03	2.05	2.45	2.64
FeCo-GDY	1.90	2.00	2.08	1.88	1.98	1.99	2.38	2.58
FeNi-GDY	1.87	1.94	2.08	1.88	1.97	1.97	2.44	2.56
FeCu-GDY	1.88	2.05	2.08	1.98	2.04	2.05	2.54	2.64
FeY-GDY	1.85	2.07	2.08	2.38	2.51	2.59	2.81	3.22
FeZr-GDY	1.85	2.06	2.08	2.23	2.43	2.48	2.58	3.07
FeNb-GDY	1.85	2.05	2.08	2.13	2.25	2.33	2.45	2.96
FeMo-GDY	1.87	1.98	2.08	2.14	2.19	2.27	2.49	2.86
FeRu-GDY	1.92	2.03	2.08	1.98	2.04	2.19	2.40	2.78
FeRh-GDY	1.91	2.03	2.08	2.00	2.11	2.15	2.43	2.74
FePd-GDY	1.90	2.01	2.08	2.07	2.07	2.12	2.47	2.71
FeHf-GDY	1.88	2.04	2.08	2.21	2.30	2.51	2.58	3.07
FeTa-GDY	1.86	2.06	2.08	2.09	2.26	2.46	2.56	3.02
FeW-GDY	1.87	1.97	2.08	2.03	2.23	2.38	2.49	2.94
FeRe-GDY	1.84	1.93	2.08	2.00	2.25	2.27	2.41	2.83
FeOs-GDY	1.93	2.03	2.08	1.95	2.01	2.20	2.43	2.76
FeIr-GDY	1.93	2.03	2.08	1.99	2.05	2.17	2.43	2.73
FePt-GDY	1.92	2.02	2.08	2.01	2.20	2.22	2.46	2.68

[a] $d_{min(Fe–C)}$ and $d_{max(Fe–C)}$ refer to the shortest and longest length between Fe atom and carbon atoms, respectively, in FeM-GDY. $d_{min(M–C)}$ and $d_{max(M–C)}$ refer to the shortest and longest length between M atom and carbon atoms, respectively, in FeM-GDY. $d_{Fe–M}$ refers to the bond length of the Fe–M in FeM-GDY. r_{Fe-C}, $r_{M–C}$, and $r_{Fe–M}$ refer to the sum of the covalent radii of the Fe and carbon atoms, the M and carbon atoms, and the Fe and M atoms, respectively.

The metal atoms are, depending on the radii of the two metal atoms, in or out of the GDY plane. Six metal atoms (i.e., Mn, Co, Ni, Cu, Pd, and Pt) form the DACs with Fe atom almost in-plane configurations, whereas the remaining 17 metals (i.e., Sc, Ti, V, Cr, Fe, Y, Zr, Nb, Mo, Ru, Rh, Hf, Ta, W, Re, Os, and

Ir) slightly protrude out of the GDY plane (~0.5–1.23 Å), leading to the slightly distortion of GDY planar structure. The metal–C bond lengths, in the range of 1.82 (Fe–C bond) to 2.51 Å (Y–C bond), are shorter than the sum of the radii of the carbon and metal atoms (2.08–2.59 Å). The distance of the two metals ranges between 2.38 (Fe–Co bond) and 2.81 Å (Fe–Y bond), also less than the sum of the radii of the two metal atoms (2.58–3.22 Å). These results indicate that there is strong interaction between the metal atoms and the sp-hybridized carbon atoms of the acetylenic ring, and between the two metal atoms, suggesting the high possibility of formation of the FeM-GDYs.

Table S2. The calculated E_b, E_c, and the experimental E_c, the charge transfer from the metal atoms to the GDY, and the spin magnetic moment of the M atoms in FeM-GDYs.[a]

FeM-GDY	E_b / eV	E_c^{cal}(M) / eV	E_c^{exp}(M) / eV	q (Fe) / $\|e^-\|$	q(M) / $\|e^-\|$	μ(Fe) / μ_B	μ(M) / μ_B
FeSc-GDY	–7.90	–4.62	–3.90	0.21	0.18	1.41	0.00
FeTi-GDY	–8.29	–5.88	–4.85	0.22	0.14	1.78	0.41
FeV-GDY	–7.51	–5.75	–5.31	0.19	0.13	1.78	1.57
FeCr-GDY	–6.45	–4.66	–4.10	0.23	0.17	1.68	2.68
FeMn-GDY	–6.47	–4.56	–2.92	0.20	0.16	2.07	3.24
FeFe-GDY	–7.25	–4.92	–4.28	0.19	0.13	2.20	2.10
FeCo-GDY	–7.71	–5.79	–4.39	0.23	0.02	2.22	1.04
FeNi-GDY	–7.56	–5.18	–4.44	0.23	0.01	2.08	0.13
FeCu-GDY	–5.68	–4.02	–4.39	0.15	0.01	1.92	0.00
FeY-GDY	–8.94	–5.03	–4.37	0.21	0.17	1.52	–0.12
FeZr-GDY	–8.32	–6.95	–6.25	0.22	0.21	1.79	0.36
FeNb-GDY	–8.32	–7.32	–7.57	0.21	0.18	1.46	–0.52
FeMo-GDY	–6.90	–6.52	–6.82	0.18	0.24	1.77	1.82
FeRu-GDY	–8.28	–7.67	–6.74	0.06	0.25	1.72	0.00
FeRh-GDY	–7.90	–6.17	–5.75	0.11	0.19	2.05	0.13
FePd-GDY	–6.50	–4.19	–3.89	0.18	0.15	2.16	0.00
FeHf-GDY	–8.54	–7.11	–6.44	0.19	0.12	1.82	3.44
FeTa-GDY	–9.21	–9.10	–8.10	0.17	0.15	1.63	0.35
FeW-GDY	–8.39	–9.02	–8.90	–	–	–	–
FeRe-GDY	–7.57	–8.65	–8.03	–	–	–	–
FeOs-GDY	–8.51	–9.28	–8.17	–	–	–	–
FeIr-GDY	–8.44	–7.40	–6.94	0.10	0.12	1.91	0.00
FePt-GDY	–7.45	–5.48	–5.84	0.21	0.10	2.16	0.00

[a] E_c^{cal}(M) and E_c^{exp}(M) refer to the theoretical calculated and experimental E_c of the M atoms. The E_c^{exp}(M) were adopted from Kittel, C. *Introduction to Solid State Physics*, Chapter 3. John Wiley & Sons, Inc., 2005. The theoretical calculated and experimental E_c for Fe atoms is –4.92 and –4.28 eV, respectively.

Table S3. The E_{ads} (in eV) of the N_2 and the intermediate in eNRR on FeM-GDYs, and the length of N–N bond (d_{N-N}, in Å) of the adsorbed N_2 molecule. [a]

FeM-GDY	*N_2(end-on)	*N_2(side-on)	$d_{N–N}$	*NNH	*NNH_2	*N	*NH	*NH_2	*NH_3	*H
FeSc-GDY	–1.51	–1.46	1.16	–2.84	–3.77	–5.03	–5.35	–4.75	–1.95	–1.00
FeTi-GDY	–1.37	–1.29	1.15	–2.95	–4.38	–5.99	–5.82	–4.90	–1.66	–1.19
FeV-GDY	–1.14	–	1.16	–3.17	–4.30	–6.21	–5.85	–4.74	–1.71	–1.04
FeCr-GDY	–0.86	–0.75	1.15	–2.82	–3.76	–5.59	–5.05	–4.22	–1.36	–0.53
FeMn-GDY	–1.04	–0.70	1.15	–2.98	–3.70	–5.22	–4.97	–4.53	–0.89	–0.92
FeFe-GDY	–0.89	–0.30	1.15	–2.87	–3.94	–5.30	–4.91	–4.01	–1.59	–0.78
FeCo-GDY	–0.54	–0.12	1.15	–2.73	–3.75	–4.93	–4.70	–3.75	–1.77	–0.68
FeNi-GDY	–0.61	–0.43	1.16	–2.75	–2.94	–4.83	–4.54	–3.91	–1.86	–0.12
FeCu-GDY	–0.9	–	1.15	–2.72	–3.23	–4.92	–4.93	–4.12	–1.88	–1.13
FeY-GDY	–1.61	–1.41	1.16	–2.79	–3.22	–5.46	–5.05	–4.86	–1.93	–1.12
FeZr-GDY	–1.33	–1.03	1.15	–2.96	–4.20	–5.97	–5.77	–4.76	–1.56	–1.02
FeNb-GDY	–1.09	–0.97	1.15	–2.95	–4.04	–6.08	–5.76	–4.37	–1.62	–0.97
FeMo-GDY	–1.13	–0.94	1.15	–3.10	–3.86	–6.33	–5.21	–4.15	–2.09	–0.84
FeRu-GDY	–0.53	–	1.15	–2.76	–3.03	–4.90	–4.72	–3.90	–1.35	–0.53
FeRh-GDY	–0.56	–	1.14	–2.60	–2.63	–5.05	–4.45	–3.54	–1.20	–0.66
FePd-GDY	–0.23	–	1.13	–1.81	–2.62	–4.02	–3.64	–2.70	–1.09	–0.33
FeHf-GDY	–1.11	–0.70	1.15	–2.85	–4.14	–5.84	–5.57	–4.46	–1.60	–0.92
FeTa-GDY	–1.08	–0.50	1.15	–3.27	–3.81	–5.79	–5.79	–5.05	–1.72	–0.64
FeIr-GDY	–0.51	–	1.15	–2.20	–3.17	–4.79	–4.68	–3.20	–1.23	–0.75
FePt-GDY	–0.21	–	1.13	–1.68	–2.40	–4.11	–3.85	–2.54	–1.47	–0.36

[a] The E_{ads} of the H adsorption on the FeM-GDYs is also included here. The $d_{N–N}$ refers to the length of the N–N bond of the adsorbed N_2 on the FeM-GDYs in an end-on adsorption configuration.

Table S4. The calculated zero-point energy (E_{ZPE}, in eV), and *TS* (in eV) of intermediate in eNRR and adsorbed H on FeM-GDYs.

FeM-GDY	*N_2		*NNH		*NNH_2		*N		*NH		*NH_2		*NH_3		*H	
	E_{ZPE}	*TS*	E_{ZPE}	*TS*	E_{ZPE}	*TS*	E_{ZPE}	*TS*	E_{ZPE}	*TS*	E_{ZPE}	*TS*	E_{ZPE}	*TS*	E_{ZPE}	*TS*
FeSc	0.23	0.11	0.50	0.13	0.83	0.14	0.09	0.04	0.37	0.05	0.71	0.07	1.06	0.11	0.19	0.01
FeTi	0.22	0.12	0.51	0.12	0.86	0.12	0.10	0.03	0.38	0.05	0.70	0.07	1.06	0.12	0.19	0.01
FeV	0.21	0.13	0.52	0.12	0.84	0.14	0.10	0.03	0.39	0.05	0.74	0.06	1.05	0.11	0.19	0.01
FeCr	0.21	0.14	0.51	0.10	0.83	0.17	0.10	0.03	0.38	0.05	0.73	0.06	1.04	0.14	0.18	0.01
FeMn	0.23	0.12	0.49	0.13	0.83	0.17	0.10	0.03	0.38	0.05	0.72	0.06	0.99	0.24	0.20	0.01
FeFe	0.22	0.12	0.53	0.10	0.86	0.11	0.10	0.03	0.38	0.05	0.74	0.05	1.04	0.15	0.22	0.01
FeCo	0.23	0.12	0.53	0.10	0.86	0.10	0.10	0.03	0.39	0.05	0.74	0.05	1.05	0.12	0.22	0.01
FeNi	0.23	0.12	0.53	0.09	0.80	0.21	0.10	0.03	0.39	0.05	0.73	0.05	1.06	0.11	0.21	0.01
FeCu	0.20	0.15	0.52	0.11	0.83	0.15	0.10	0.04	0.40	0.05	0.75	0.06	1.06	0.11	0.21	0.01
FeY	0.18	0.16	0.50	0.11	0.79	0.18	0.10	0.04	0.36	0.06	0.73	0.07	1.06	0.11	0.19	0.01
FeZr	0.23	0.12	0.52	0.11	0.84	0.12	0.10	0.03	0.37	0.05	0.71	0.07	1.07	0.10	0.18	0.01
FeNb	0.21	0.14	0.52	0.12	0.82	0.17	0.10	0.03	0.37	0.06	0.71	0.07	1.04	0.14	0.21	0.01
FeMo	0.20	0.16	0.52	0.10	0.79	0.23	0.10	0.04	0.39	0.05	0.68	0.08	1.02	0.20	0.17	0.01
FeRu	0.22	0.13	0.53	0.10	0.84	0.14	0.09	0.03	0.37	0.05	0.73	0.05	1.05	0.11	0.21	0.01
FeRh	0.21	0.14	0.53	0.10	0.85	0.12	0.10	0.03	0.37	0.06	0.76	0.05	1.05	0.13	0.20	0.01
FePd	0.19	0.18	0.51	0.11	0.81	0.16	0.10	0.04	0.37	0.06	0.74	0.06	1.03	0.16	0.23	0.00
FeHf	0.22	0.13	0.51	0.11	0.83	0.15	0.10	0.03	0.38	0.06	0.73	0.06	1.06	0.11	0.21	0.01
FeTa	0.21	0.13	0.51	0.12	0.83	0.15	0.10	0.03	0.39	0.05	0.73	0.07	1.06	0.13	0.19	0.01
FeIr	0.21	0.13	0.50	0.13	0.83	0.13	0.09	0.04	0.38	0.06	0.77	0.04	1.05	0.13	0.22	0.01
FePt	0.18	0.11	0.49	0.14	0.81	0.15	0.10	0.04	0.38	0.05	0.72	0.06	1.01	0.22	0.22	0.01

Table S5. The calculated Δ*G* (in eV) of each intermediate and adsorbed H on FeM-GDYs.[a]

FeM-GDY	*N_2	*NNH	*NNH_2	*NH	*NH_2	*NH_3	*H	*H on bulk M
FeSc-GDY	–0.94	–2.15	–3.08	–4.70	–4.04	–1.30	–0.75	–0.83
FeTi-GDY	–0.82	–2.24	–3.64	–5.16	–4.20	–1.02	–0.93	–0.97
FeV-GDY	–0.60	–2.45	–3.59	–5.18	–3.99	–1.07	–0.78	–0.79
FeCr-GDY	–0.33	–2.08	–3.10	–4.38	–3.48	–0.76	–0.29	–0.50
FeMn-GDY	–0.48	–2.15	–3.03	–4.30	–3.80	–0.44	–0.67	–0.92
FeFe-GDY	–0.44	–2.11	–3.19	–4.24	–3.16	–1.00	–0.50	–0.48
FeCo-GDY	–0.12	–1.98	–2.99	–4.03	–2.99	–1.14	–0.39	–0.28
FeNi-GDY	–0.15	–1.99	–2.35	–3.86	–3.16	–1.21	0.15	–0.25
FeCu-GDY	–0.39	–1.99	–2.55	–4.24	–3.36	–1.23	–0.65	–0.07
FeY-GDY	–1.09	–2.07	–2.61	–4.42	–4.13	–1.28	–0.87	–0.96
FeZr-GDY	–0.77	–2.22	–3.48	–5.12	–4.04	–0.89	–0.77	–1.04
FeNb-GDY	–0.56	–2.21	–3.39	–5.11	–3.66	–1.02	–0.69	–0.73
FeMo-GDY	–0.64	–2.35	–3.29	–4.56	–3.49	–1.57	–0.61	–0.45
FeRu-GDY	–0.01	–2.00	–2.33	–4.06	–3.15	–0.71	–0.26	–0.45
FeRh-GDY	–0.04	–1.84	–1.90	–3.80	–2.76	–0.58	–0.40	–0.54
FePd-GDY	0.24	–1.09	–1.96	–3.00	–1.95	–0.52	–0.03	–0.53
FeHf-GDY	–0.49	–2.15	–3.43	–4.95	–3.57	–0.95	–0.64	–1.14
FeTa-GDY	–0.46	–1.75	–3.11	–5.19	–4.16	–1.09	–0.38	–0.68
FeIr-GDY	–0.02	–1.50	–2.47	–4.02	–2.65	–0.61	–0.47	–0.27
FePt-GDY	0.19	–1.00	–1.73	–3.19	–1.81	–0.98	–0.07	–0.25

[a] The Δ*G* of the H adsorption process on the bulk metal surface is also included here.

Table S6. The calculated FE on FeM-GDYs.

FeM-GDY	**FE%**
FeSc-GDY	~100
FeTi-GDY	1
FeV-GDY	0
FeCr-GDY	82
FeMn-GDY	6
FeFe-GDY	9
FeCo-GDY	0
FeNi-GDY	~100
FeCu-GDY	0
FeY-GDY	~100
FeZr-GDY	50
FeNb-GDY	1
FeMo-GDY	76
FeRu-GDY	0
FeRh-GDY	0
FeHf-GDY	0
FeTa-GDY	9
FeIr-GDY	0

3. Figures

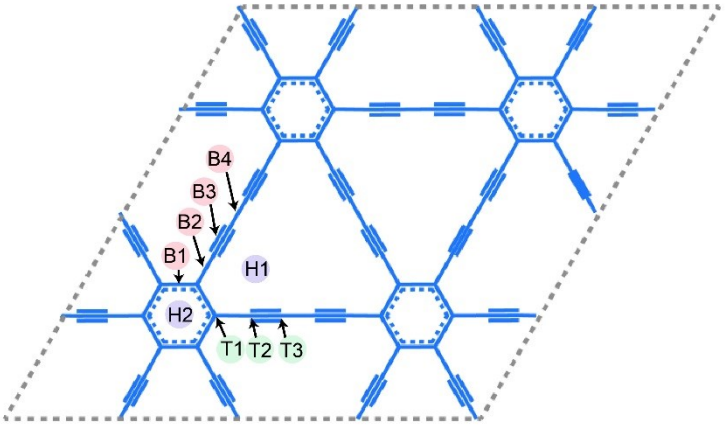

Fig. S1 Illustration the possible sites on the GDY sheet for metal atoms binding. Nine different possible binding sites including two hollow sites: H1 the hollow site above the corner of the acetylenic ring, and H2 the hollow site above the top of the hexatomic ring; three top sites: the top of three different carbon (T1, T2 and T3); four bridge sites: the top of the C−C bond (B1, B2, B3, and B4).

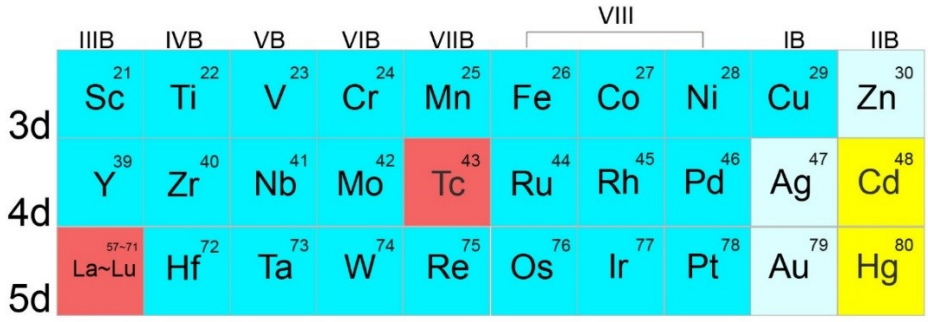

Fig. S2 Illustration of the metal atoms studied to form the FeM-GDYs. All 3d, 4d, and 5d group metal atoms, except for the lanthanides, radioactive Tc, and toxic Cd and Hg, have been induced to form the DACs with Fe atom on GDY.

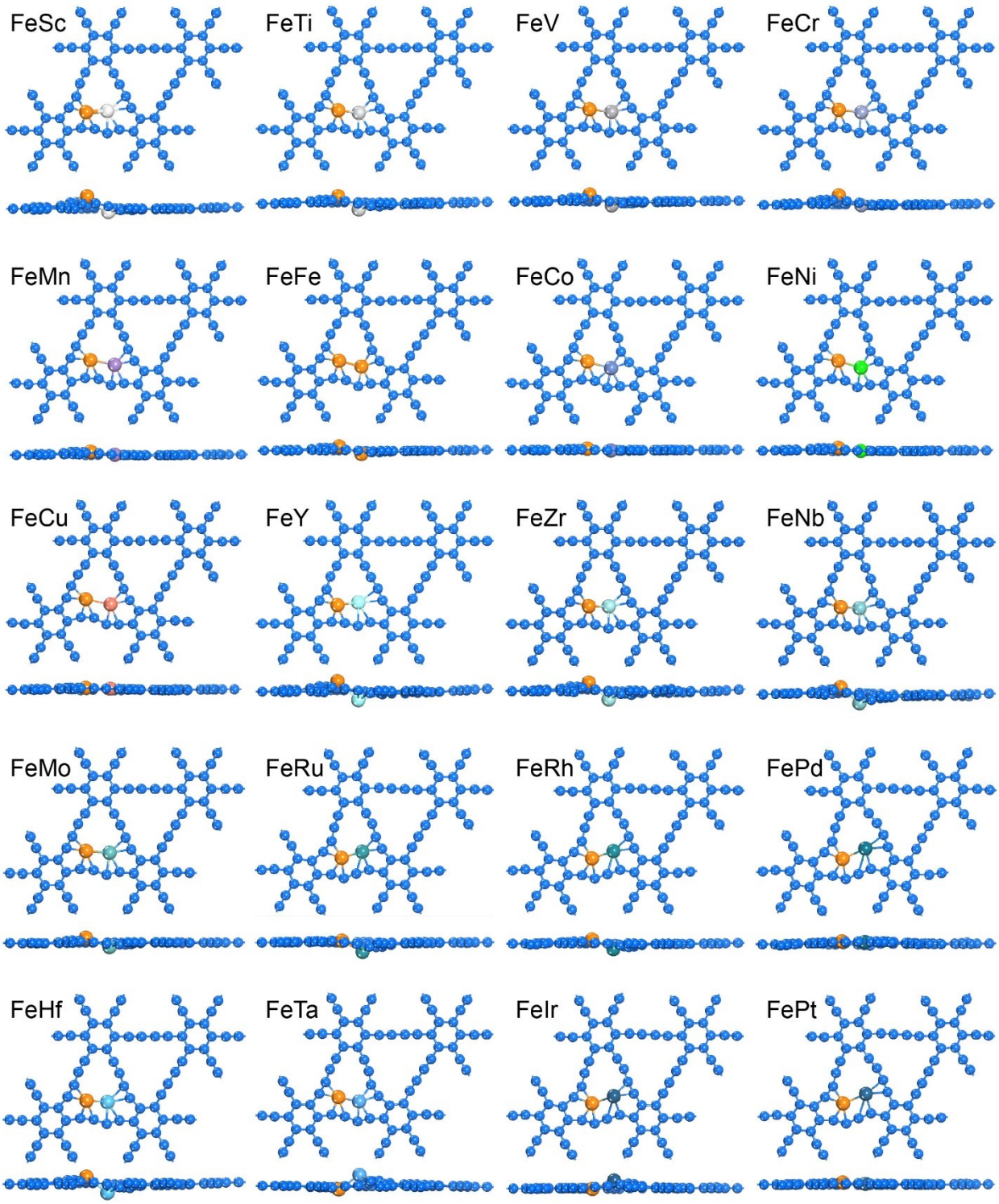

Fig. S3 The top- and side-view of the optimized structures of the FeM-GDYs (M = Sc, Ti, V, Cr, Mn, Fe, Co, Ni, Cu, Y, Zr, Nb, Mo, Ru, Rh, Pd, Hf, Ta, Ir, and Pt)

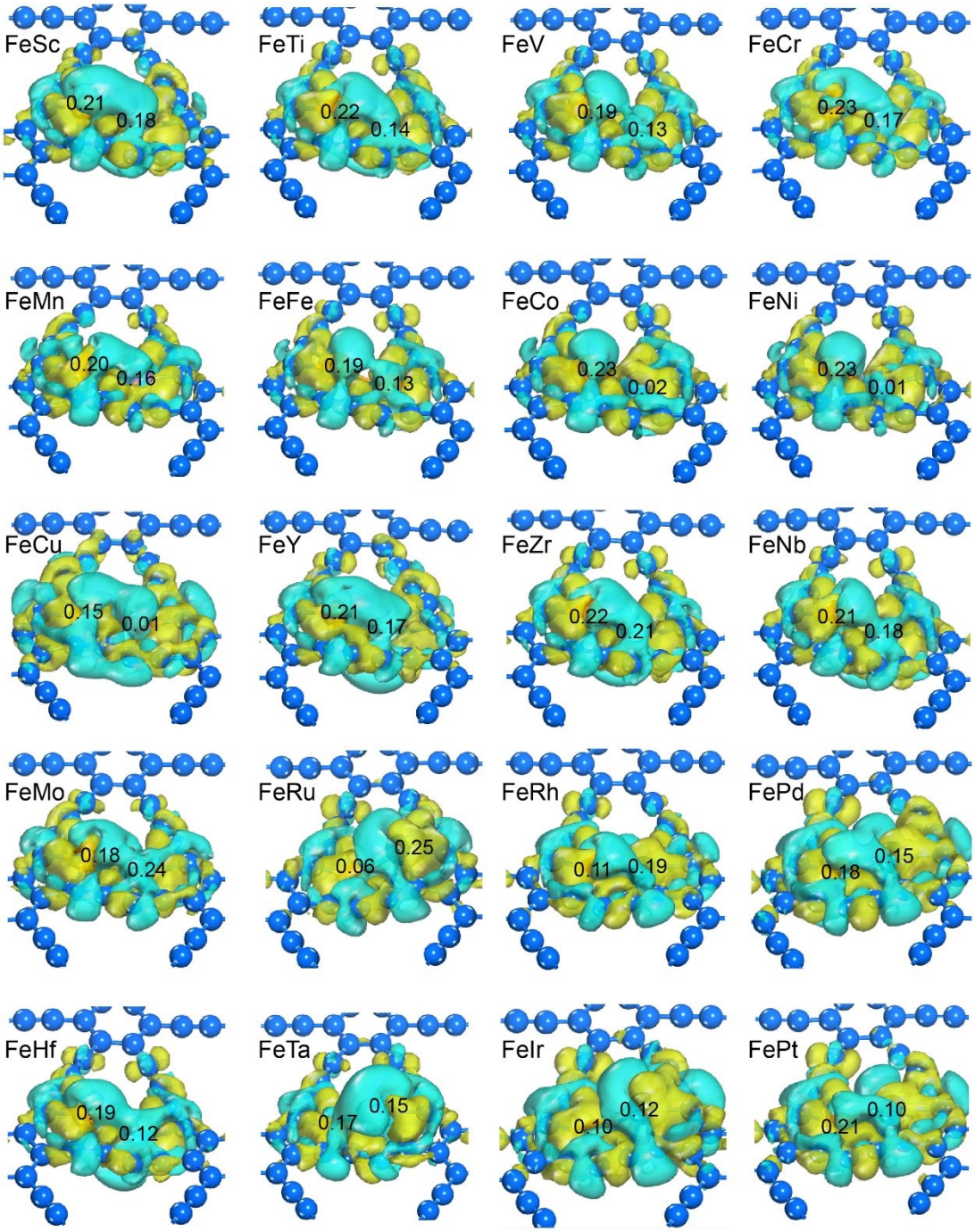

Fig. S4 The differential charge density distribution on FeM-GDYs (M = Sc, Ti, V, Cr, Mn, Fe, Co, Ni, Cu, Y, Zr, Nb, Mo, Ru, Rh, Pd, Hf, Ta, Ir, and Pt). The isosurface value is ~0.008e^{-}Å^{-3}. The charge accumulation and depletion is denoted by yellow and cyan colors, respectively. The number in the panels refers the charges transferred to carbon atoms from each metals.

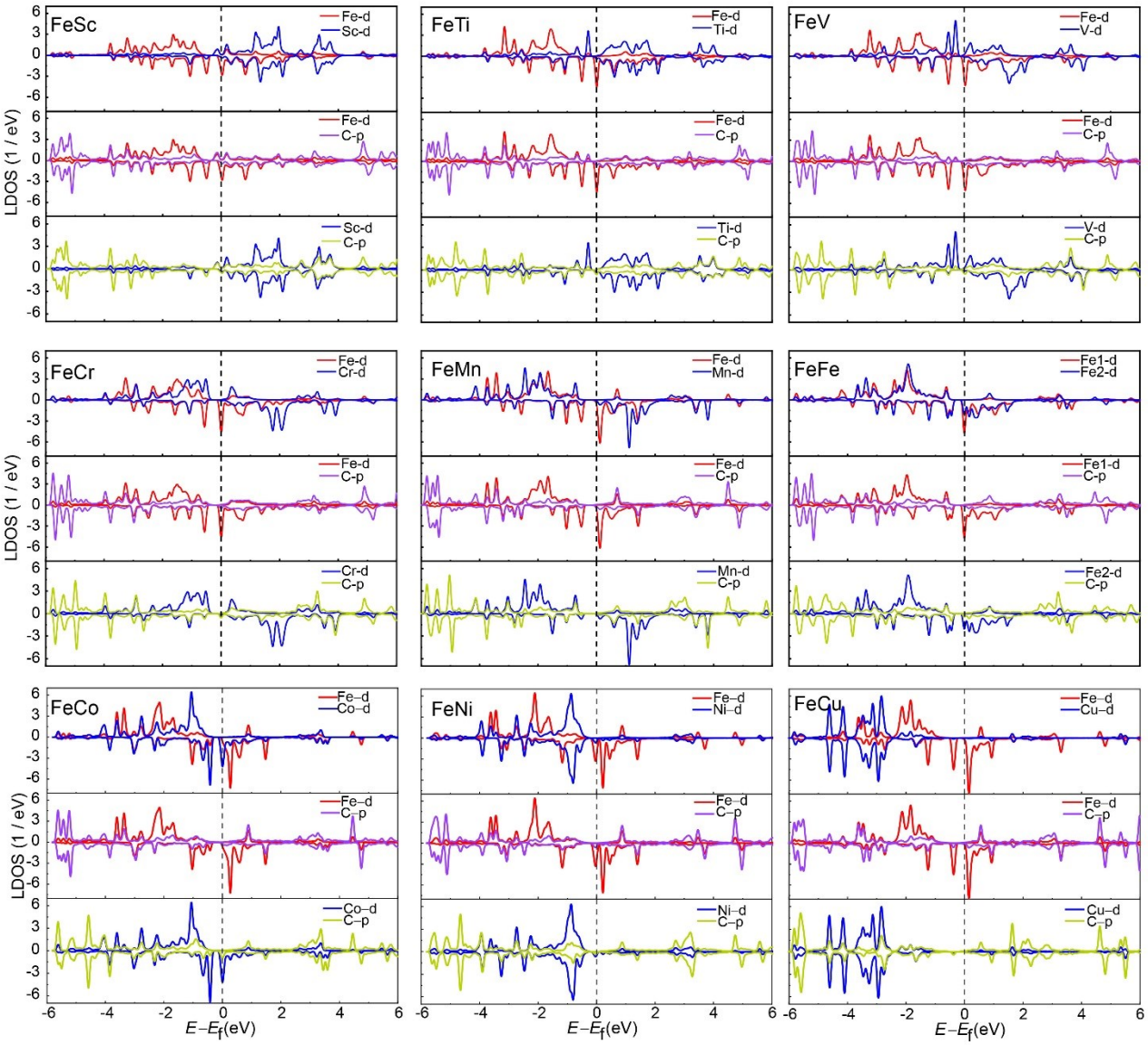
FeSc
Fe-d
Sc-d
Fe-d
C-p
Sc-d
C-p
FeTi
Fe-d
Ti-d
Fe-d
C-p
Ti-d
C-p
FeV
Fe-d
V-d
Fe-d
C-p
V-d
C-p
FeCr
Fe-d
Cr-d
Fe-d
C-p
Cr-d
C-p
FeMn
Fe-d
Mn-d
Fe-d
C-p
Mn-d
C-p
FeFe
Fe1-d
Fe2-d
Fe1-d
C-p
Fe2-d
C-p
FeCo
Fe–d
Co–d
Fe–d
C–p
Co–d
C–p
FeNi
Fe–d
Ni–d
Fe–d
C–p
Ni–d
C–p
FeCu
Fe–d
Cu–d
Fe–d
C–p
Cu–d
C–p
LDOS (1 / eV)
E–Ef(eV)

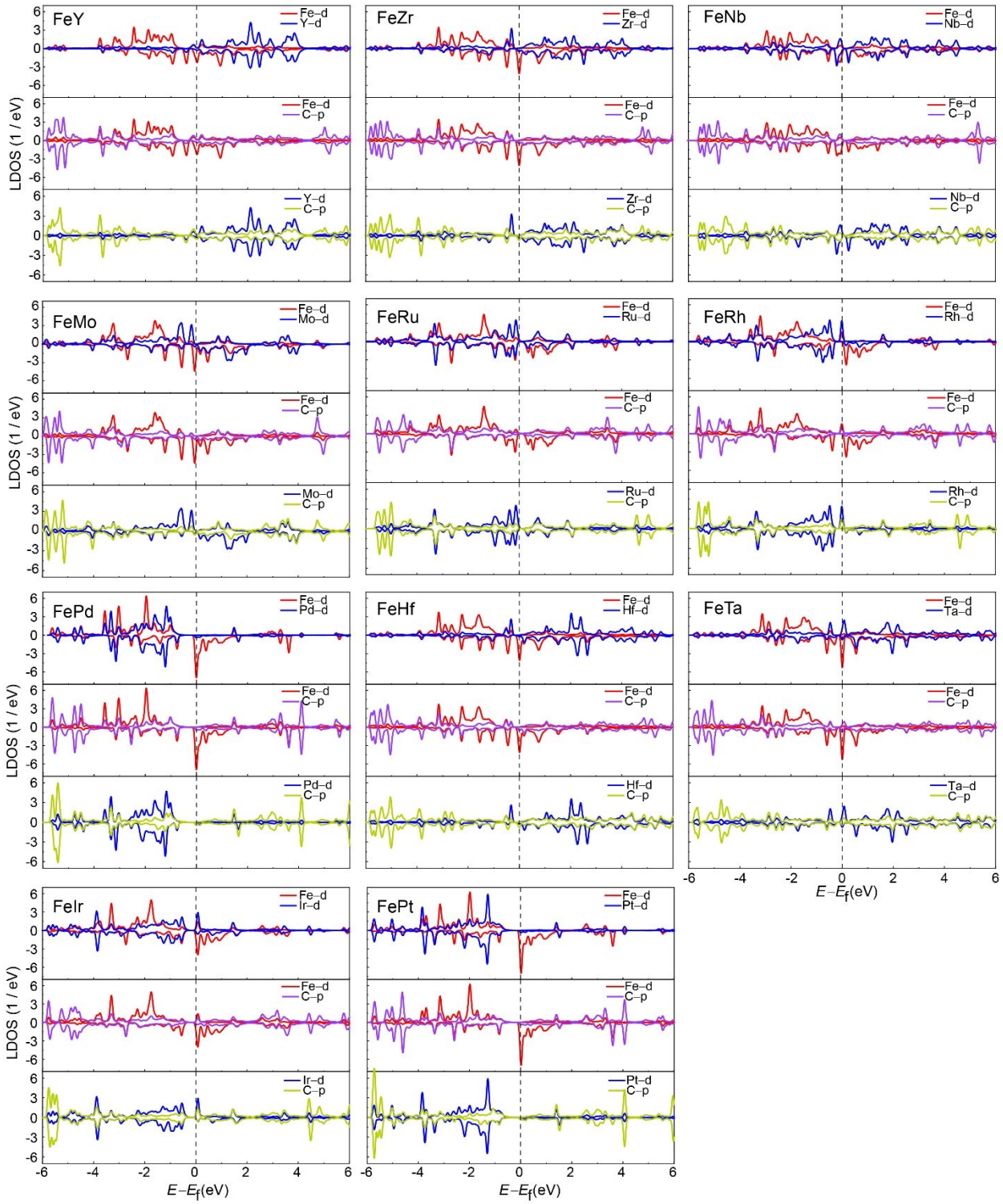

Fig. S5 LDOS of FeM-GDYs (M = Sc, Ti, V, Cr, Mn, Fe, Co, Ni, Cu, Y, Zr, Nb, Mo, Ru, Rh, Pd, Hf, Ta, Ir, and Pt).

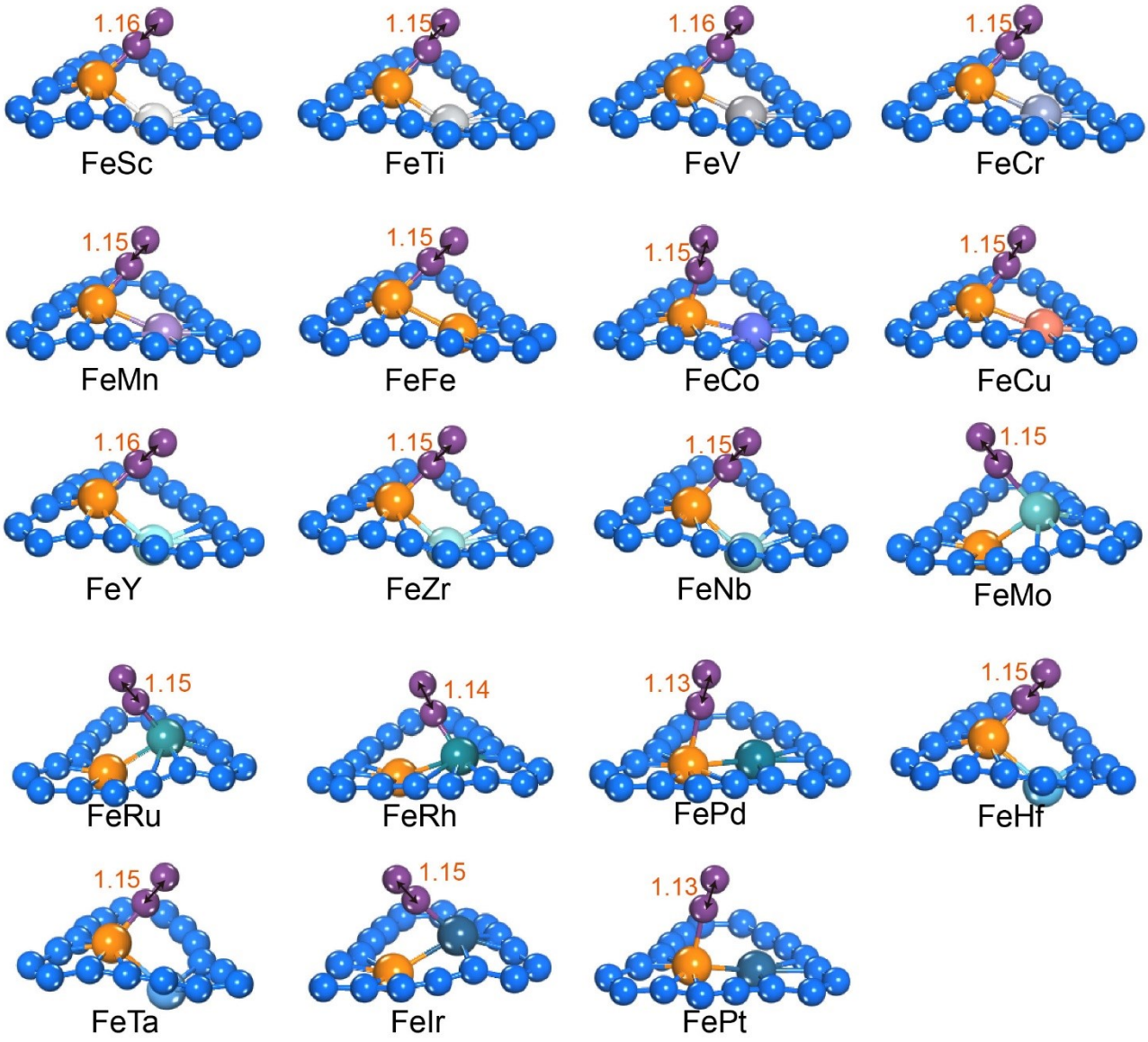

Fig. S6 The configurations of N_2 adsorbed on (end-on) the FeM-GDYs (M = Sc, Ti, V, Cr, Mn, Fe, Co, Cu, Y, Zr, Nb, Mo, Ru, Rh, Pd, Hf, Ta, Ir, and Pt). The red number indicates the bond length (in Å) of adsorbed N_2.

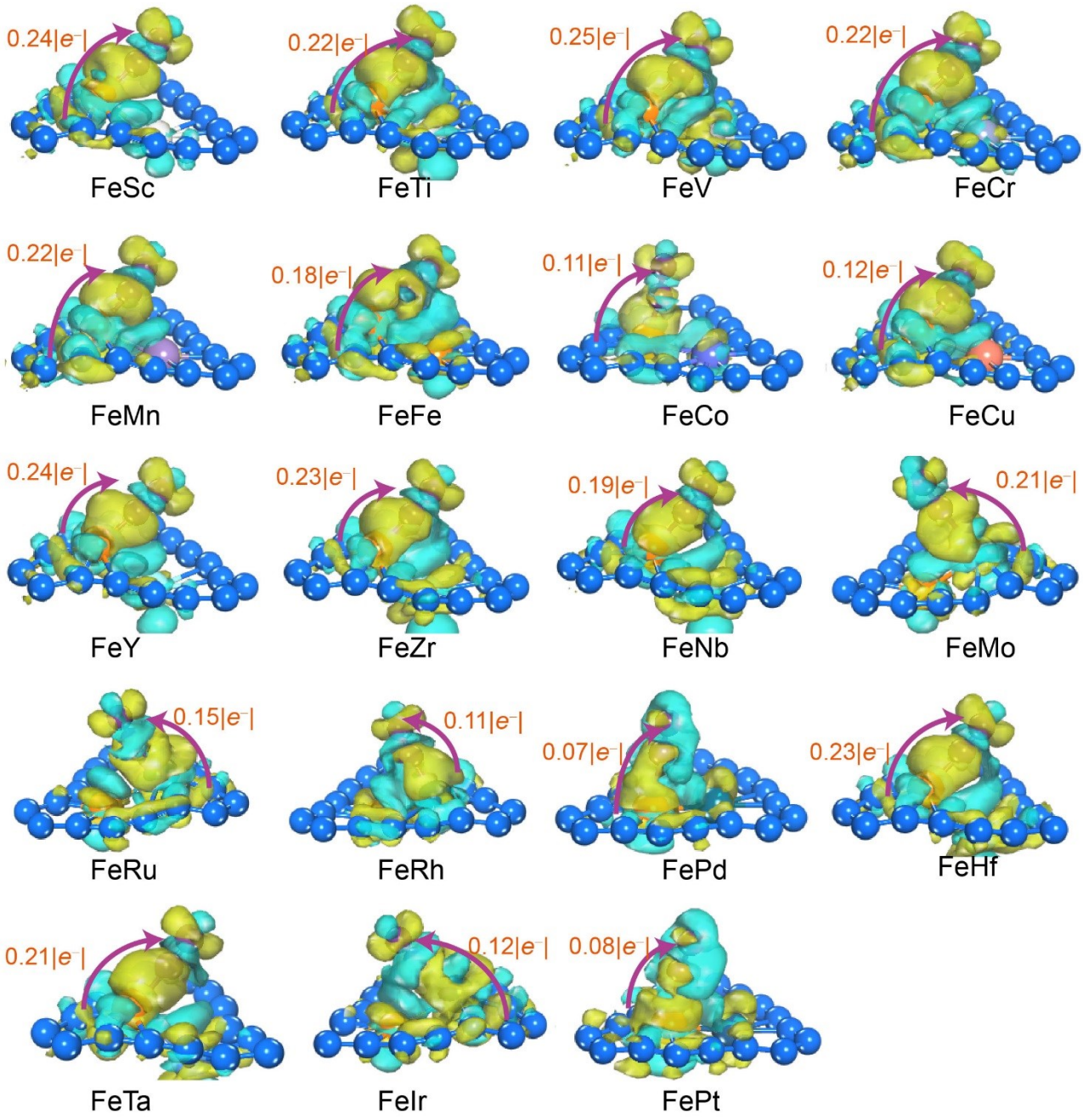

Fig. S7 The charge density differences of N_2 adsorbed on the FeM-GDYs (M = Sc, Ti, V, Cr, Mn, Fe, Co, Cu, Y, Zr, Nb, Mo, Ru, Rh, Pd, Hf, Ta, Ir, and Pt). The charge accumulation and depletion are depicted by yellow and cyan, respectively. The isosurface value is 0.005 e^- Å^{-3}.

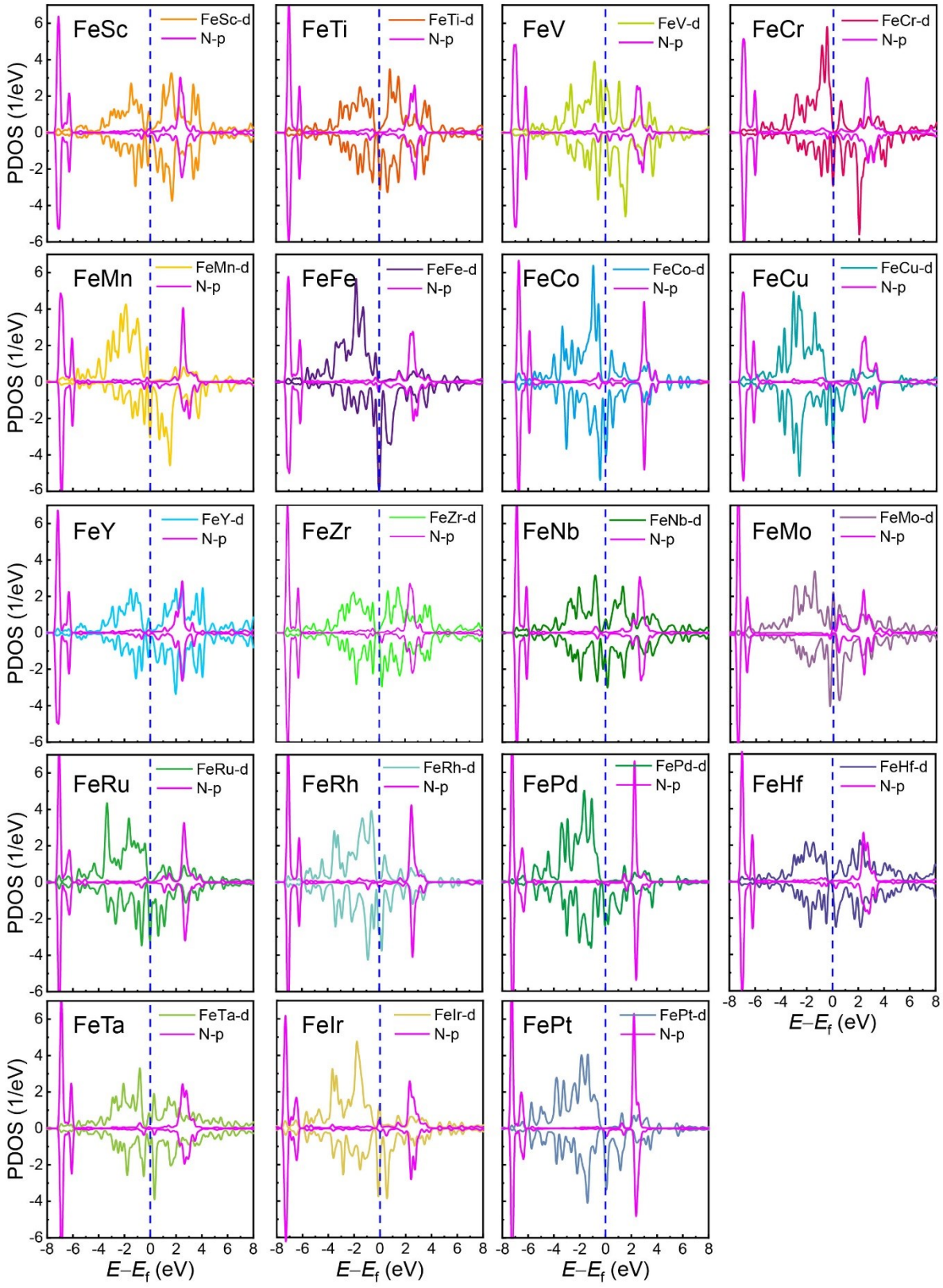

Fig. S8 PDOS of the *N_2-2p and FeM-3d in the N_2-adsorbed FeM-GDYs (M = Sc, Ti, V, Cr, Mn, Fe, Co, Cu, Y, Zr, Nb, Mo, Ru, Rh, Pd, Hf, Ta, Ir, and Pt) system.

Fig. S9 The optimized adsorption configurations of each intermediate in eNRR on FeM-GDYs (M = Sc, Ti, V, Cr, Mn, Fe, Co, Ni, Cu, Y, Zr, Nb, Mo, Ru, Rh, Hf, Ta, and Ir).

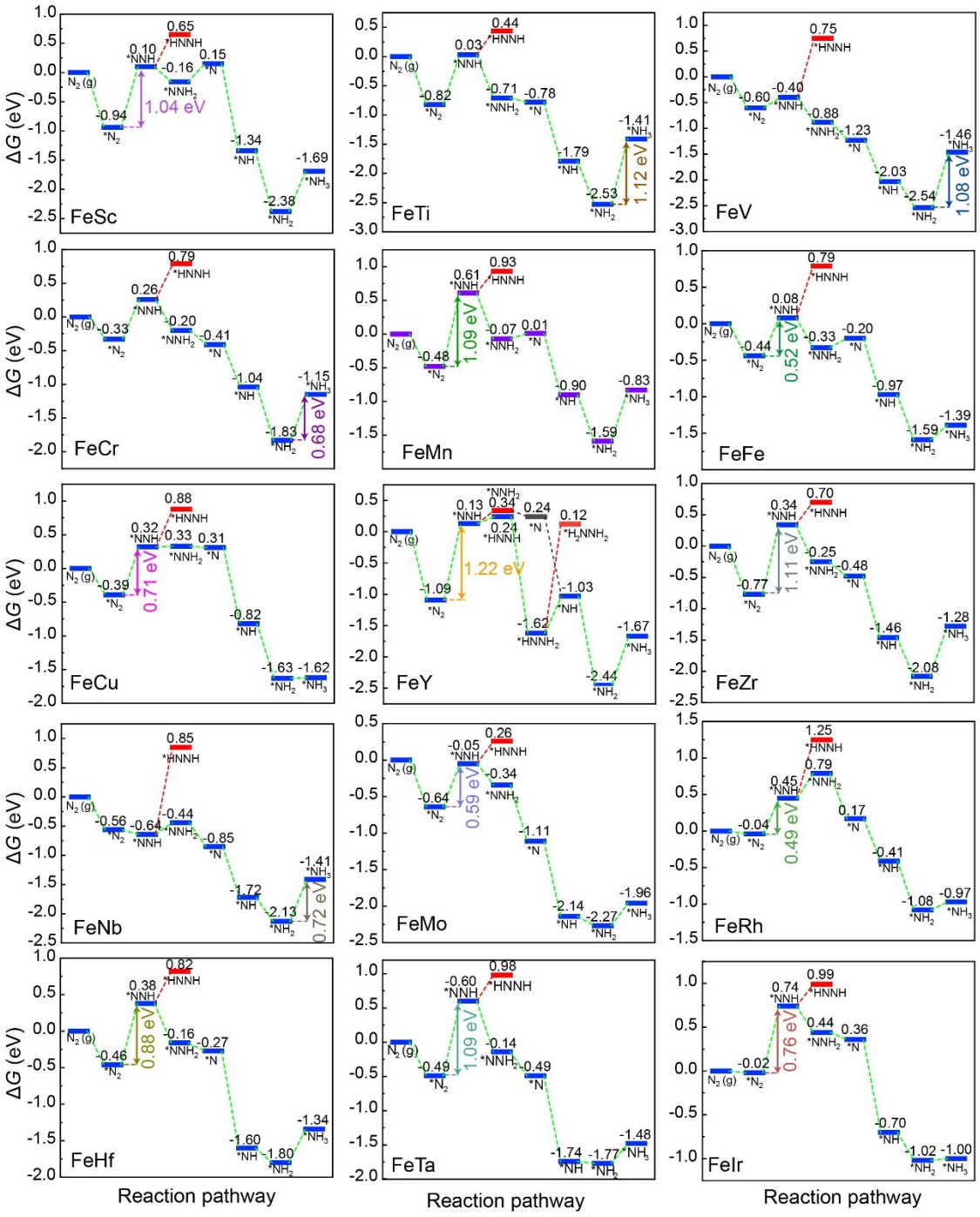

Fig. S10 The free energy diagrams of the eNRR on FeM-GDYs (M = Sc, Ti, V, Cr, Mn, Fe, Cu, Y, Zr, Nb, Mo, Rh, Hf, Ta, and Ir).

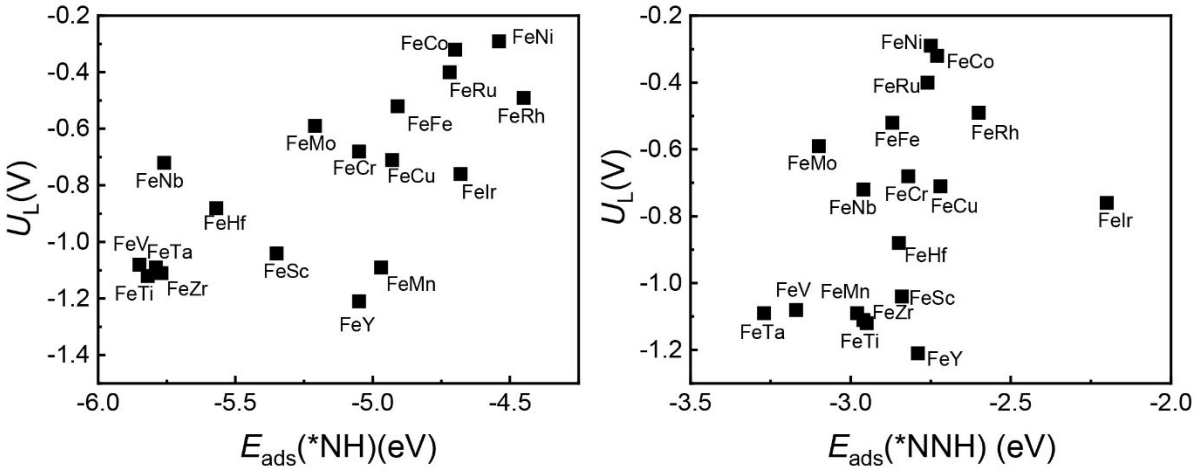

Fig. S11 Correlation between U_L and E_{ads} of (a) *NH and (b) *NNH.

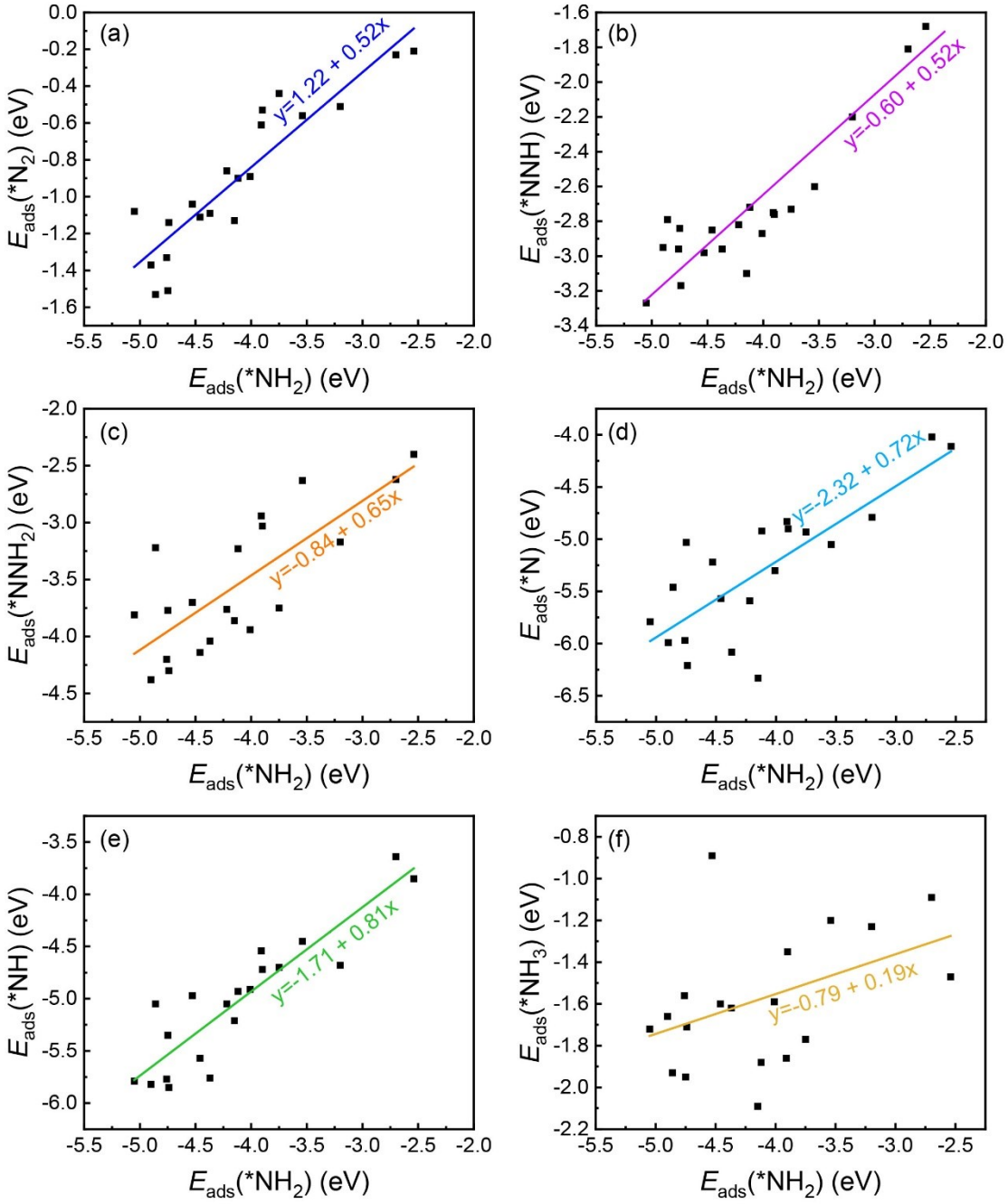

Fig. S12 Linear correlations between the adsorption energy of intermediates and E_{ads}(*NH$_2$).

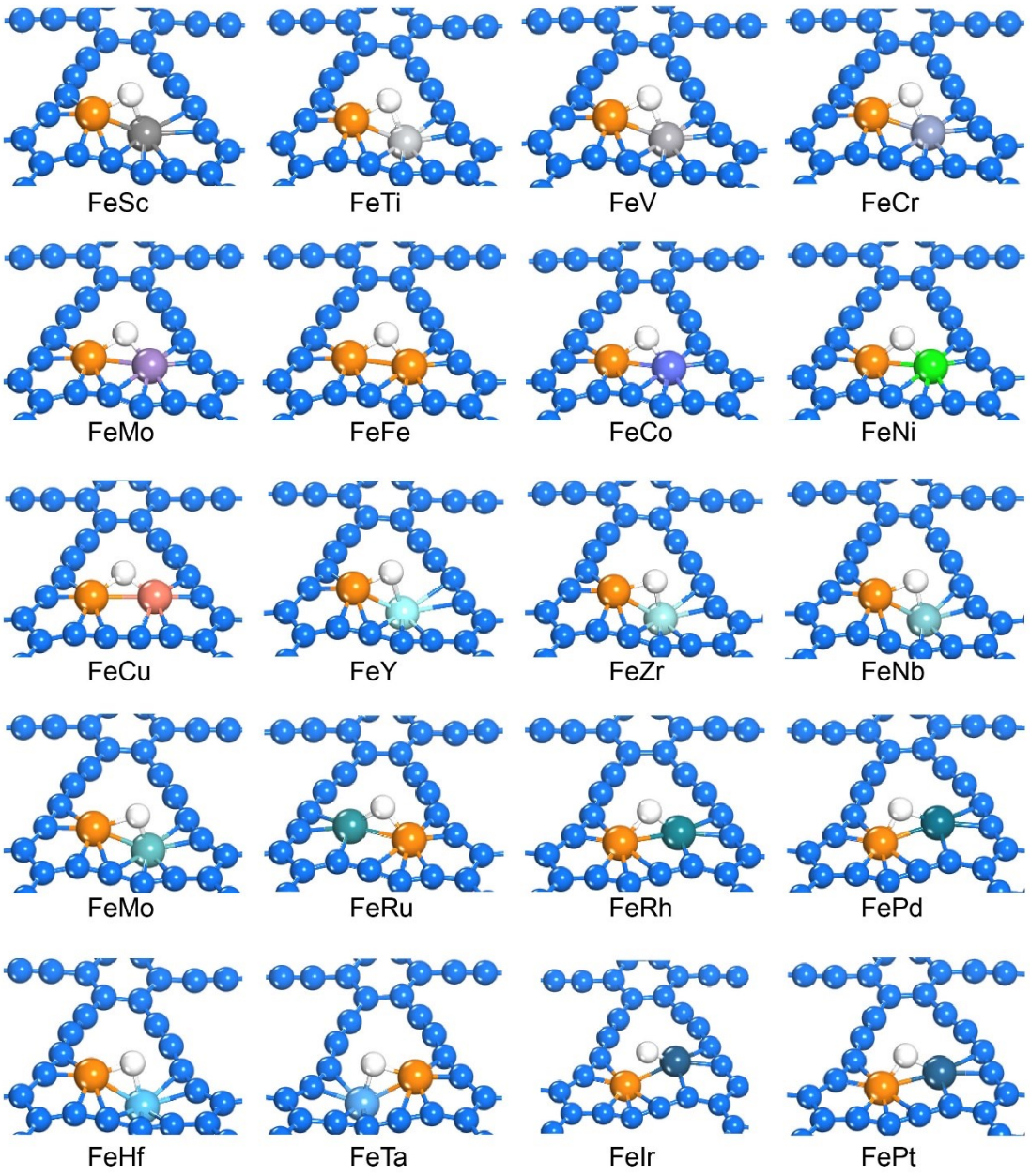

Fig. S13 The adsorption configurations of the H on the FeM-GDYs (M = Sc, Ti, V, Cr, Mn, Fe, Co, Ni, Cu, Y, Zr, Nb, Mo, Ru, Rh, Hf, Ta, and Ir).

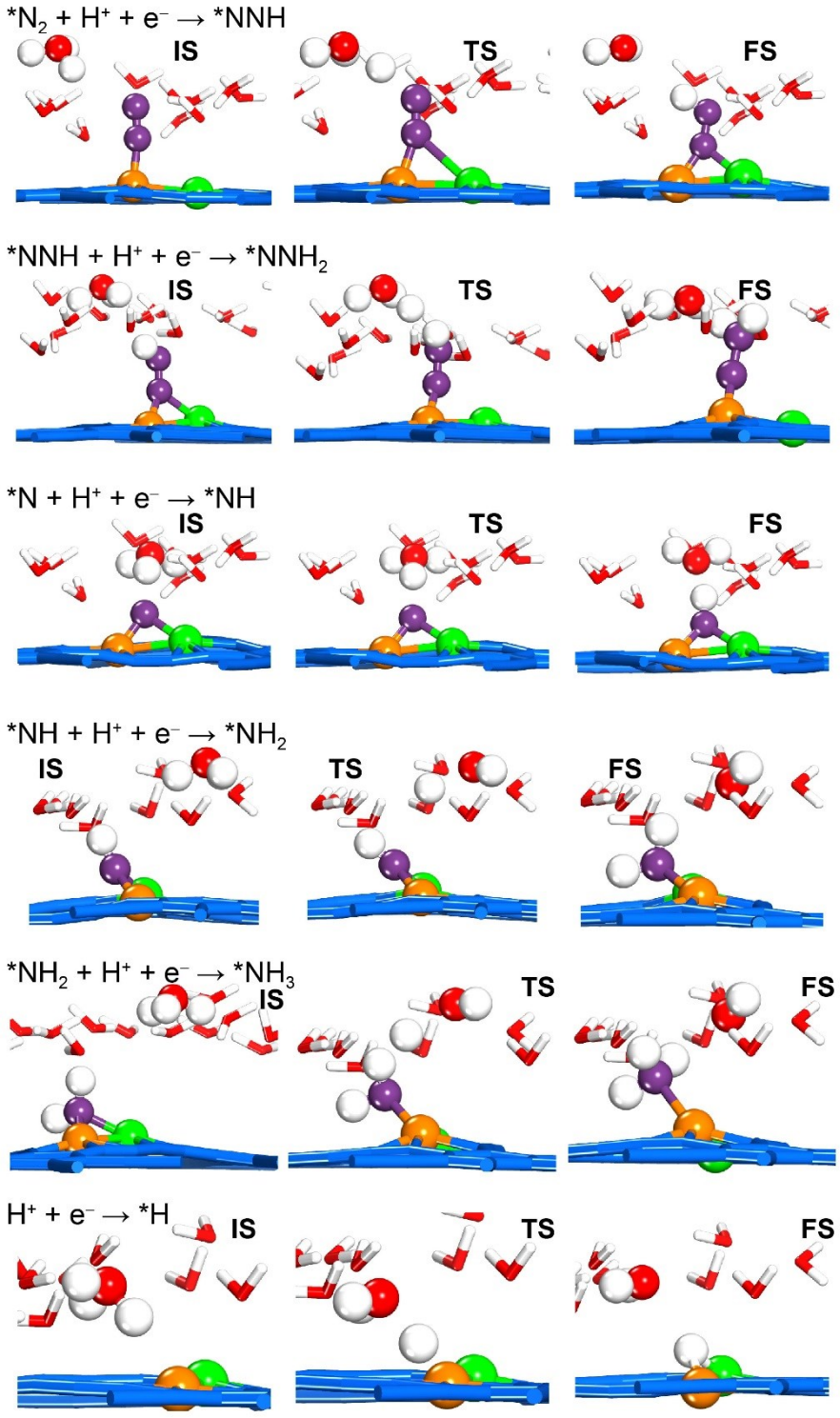

Fig. S14 Geometric structures of IS, TS and FS in each elementary reaction of eNRR and HER on FeNi-GDY. Note that for the reaction of $*NNH_2 + H^+ + e^- \rightarrow *N + NH_3$, there is no TS found according to the results of LST/QST.